JOC Article

Carbon Protonation of 2,4,6-Triaminopyrimidines: Synthesis, NMR Studies, and Theoretical Calculations

Balázs Németh,[‡] Csaba Wéber,[†] Tamás Veszprémi,[‡] Tamás Gáti,[†] and Ádám Demeter*[,†]

Department of Inorganic Chemistry, Budapest University of Technology and Economics, Gellért tér 4, H-1521 Budapest, Hungary, and Gedeon Richter Ltd., H-1475 Budapest, P.O. Box 27, Hungary

a.demeter@richter.hu

Received March 14, 2006

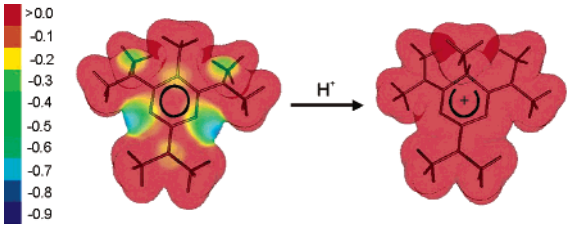

Several C(5)-substituted 2,4,6-triaminopyrimidine derivatives and their HBF_4 salts were synthesized to study the carbon protonation of the pyrimidine ring. NMR investigations in DMSO-d_6 prove experimentally that, in addition to the usual protonation at N(1), the compounds can be protonated at C(5) as well. We present several new stable cationic σ-complexes in the pyrimidine series, where C(5) protonation predominates over N(1) protonation. Quantum chemical calculations using the B3LYP/cc-pVDZ method were utilized in the gas phase and also in DMSO solvent with the polarized continuum model (PCM) method to rationalize the observed protonation behavior. Results of the calculations accord with the experimental observations and prove that combined steric and electronic effects are responsible for the observed C(5) protonation and for σ-complex stability. We demonstrate that C(5) protonation is a general feature of the 2,4,6-triaminopyrimidine system.

Introduction

The biological importance of the pyrimidine system has induced extensive research toward the understanding of structure−activity relationships.[1] Substituted 2,4-diaminopyrimidines (e.g., pyrimethamine and thrimethoprim), as well as the respective heterocyclic analogues (e.g., piritrexim and methotrexate), constitute a class of pharmacologically important dihydrofolate reductase (DHFR) inhibitors.[2] Substituted diaminopyrimidines are also known as strong AGAT inhibitors.[3] Furthermore, hexaalkyl-2,4,6-triaminopyrimidines constitute important subunits of 21-aminosteroids (e.g., tirilazad) and 2-(aminomethyl)-chromans that inhibit iron-dependent lipid peroxidation and protect against central nervous system (CNS) trauma.[4] Protonation studies might provide basic insight into the mechanism of action as clearly demonstrated for DHFR inhibitors.[5] A number of experimental and theoretical studies explored the site of protonation for simple aminopyrimidine derivatives. They indicated that protonation occurs at the pyrimidine ring nitrogen [N(1) and/or N(3)] and/or at the exocyclic amino group both in the gas phase and in solution.[6]

Recently, we have discovered that hexamethyl-2,4,6-triaminopyrimidine (**4**) (see Chart 1) could be protonated at the C(5) position in water, leading to an equilibrium between the C(5)

* To whom correspondence should be addressed. Phone: +36-1-431 5922. Fax: +36−1−431 6006.
‡ Budapest University of Technology and Economics.
† Gedeon Richter Ltd.

(1) For a comprehensive review of pyrimidines, see: (a) Brown, D. J.; Evans, R. F.; Cowden, W. B.; Fenn, M. D. *The Pyrimidines*; Wiley-Interscience: New York, 1994. (b) *Comprehensive Heterocyclic Chemistry*; Katritzky, A. R., Rees, C. W., Scriven, E. F., Eds.; Pergamon: Oxford, 1996; Vol. 6, pp 93−233. (c) *Comprehensive Heterocyclic Chemistry*; Katritzky, A. R., Rees, C. W., Eds.; Pergamon: Oxford, 1984; Vol. 3, pp 57−157.

(2) (a) Hitchings, G. H. *Angew. Chem., Int. Ed. Engl.* **1989**, *28*, 879−885. (b) Hitchings, G. H. *Rev. Port. Farm.* **1991**, *41*, 21−29. (c) Zink, M.; Lanig, H.; Troschütz, R. *Eur. J. Med. Chem.* **2004**, *39* (12), 1079−1088. (d) Gangjee, A.; Zeng, Y.; McGuire, J. J.; Kisliuk, R. J. *J. Med. Chem.* **2005**, *48* (16) 5329−5336 and references therein.

(3) Terashima, I.; Kohda, K. *J. Med. Chem.* **1998**, *41*, 503−508.

(4) (a) Jacobsen, E. J.; VanDoornik, F. J.; Ayer, D. E.; Belonga, K. L.; Braughler, J. M.; Hall, E. D.; Houser, D. J. *J. Med. Chem.* **1992**, *35*, 4464−4472. (b) Jacobsen, E. J.; McCall, J. M.; Ayer, D. E.; VanDoornik, F. J.; Palmer, J. R.; Belonga, K. L.; Braughler, J. M.; Hall, E. D.; Houser, D. J.; Krook, M. A.; Runger, T. A. *J. Med. Chem.* **1990**, *33*, 1145−1151.

(5) Feeney, K. *Angew. Chem., Int. Ed.* **2000**, *39*, 290−312.

10.1021/jo0605703 CCC: $33.50
Published on Web 06/02/2006

CHART 1

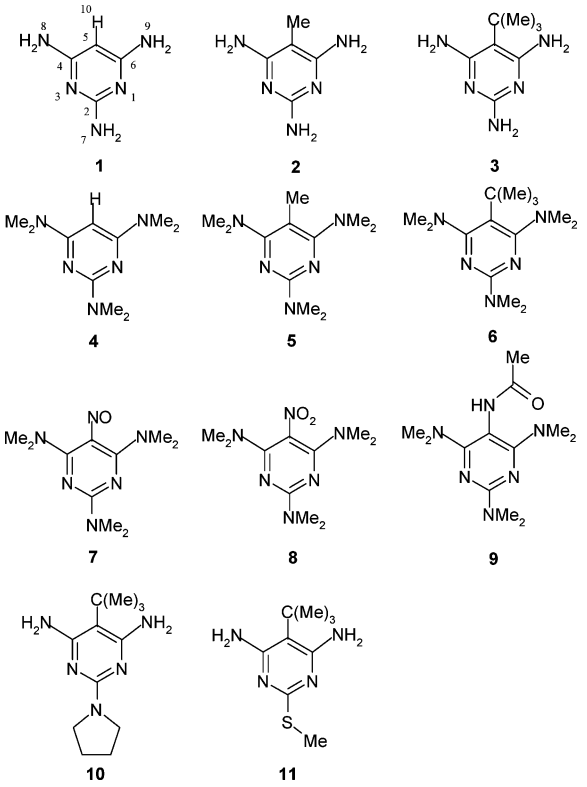

and N(1) protonated forms.[7] We have also shown that a sterically congested 1,1-bis(pyrimidin-5-yl)-2-chloroethene-type derivative is, peculiarly, fully monoprotonated at the C(5) position and forms a stable cationic σ-complex. A detailed NMR analysis with an emphasis on the story behind our structural conclusions regarding C(5) protonation has also been given.[8] We proposed that both steric and electronic effects might be responsible for the observed C(5) protonation, and they could account for the stability of the σ-complex in the bispyrimidine derivative.

To explore these effects in detail, we initiated a systematic study of the protonation behavior of the 2,4,6-triaminopyrimidine system by NMR and quantum chemical calculations. To this end, we synthesized a selected set of simple C(5)-substituted 2,4,6-triaminopyrimidine derivatives (Chart 1) and their respective HBF_4 salts. Compound **6** was failed to be prepared and was only theoretically studied. Our ultimate goal was to find new stable cationic σ-complexes among simple triaminopyrimidines and to provide experimental and theoretical evidence for their stability.

More than a hundred years after its first synthesis (1899),[9] we show a so far unexplored chemical character of the pyrimidine ring.

CHART 2

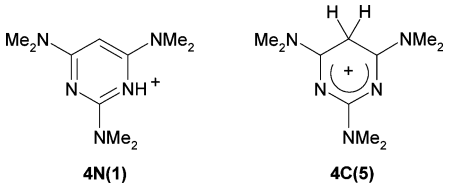

SCHEME 1[a]

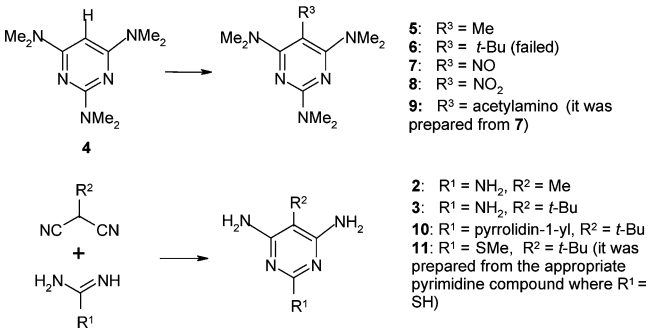

[a] Reagents and conditions. **5**: MeI (5 equiv), CH_2Cl_2, 40 °C, 120 h. **6**: A method, *t*-BuI (3 equiv), DIPEA (3 equiv), THF, 8 h, 65 °C; A method, isobutene, cat. *p*-TsOH, 65 °C, 8 h. **7**: $NaNO_2$ (2 equiv), CH_2Cl_2−AcOH−H_2O, 0−5 °C, 1 h. **8**: $NO_2BF_4 \cdot Et_2O$ (2.3 equiv), CH_2Cl_2, −70 °C, 4 h then room temperature for 24 h. **9** (from **7**): H_2, Pd/C (20%), Ac_2O (3 equiv), THF, room temperature, 3 h. **10**: NaO^tBu (1.05 equiv), EtOH, reflux, 8 h. **11**: NaO^tBu (0.97 equiv), EtOH, reflux, 8 h.

Results and Discussion

The investigated molecules and the numbering of atoms are shown in Chart 1. Throughout this paper, the protonated forms are denoted with the site of protonation after the number assigned to each molecule. For example, **4N(1)** denotes molecule **4** (base form) that is protonated at N(1), and **4C(5)** stands for the C(5) protonated form (Chart 2). Accordingly, e.g., the signal of N(1) of compound **4** corresponds to the ^{15}N NMR chemical shift of the nitrogen on position 1. Because most of the base forms of the investigated molecules are practically insoluble in water, the protonation behavior was investigated in dimethyl sulfoxide (DMSO) with the respective HBF_4 salts. HBF_4 was chosen for this study to obtain sharp NMR signals.

Synthesis. 1, **2** and **4** as well as the HBF_4 salt of **1** are known compounds,[10] and **3**, **5**, and **7**−**11** as well as the respective HBF_4 salts of **2**−**5** and **7**−**11** are newly synthesized in the pyrimidine series.

Two different approaches were used for the synthesis of 5-substituted 2,4,6-triaminopyrimidines (Scheme 1). First, 5-substituted 2,4,6-tris(dimethylamino)pyrimidines were synthesized by reaction of **4** with the appropriate electrophiles.[11] Second, in the case of 5-substituted 4,6-di- and 2,4,6-triaminopyrimidines, condensation of the respective malonitrile and amidine derivatives proved to be successful. A detailed description of the applied reaction conditions and the method of preparation is given in the Experimental Section.

It is interesting to note that methylation of **4** with iodomethane afforded a 2:1 mixture of N(7)- and C(5)-methylated products

(6) (a) Threadgill, M. D.; Griffin, R. J.; Stevens, M. F. G.; Wong, S. K. *J. Chem. Soc., Perkin Trans. I* **1987**, 2229−2234. (b) Städeli, W.; Philipsborn, W.; Wick, A.; Kompis, I. *Helv. Chim. Acta* **1980**, *63*, 504−522. (c) Riand, J.; Chenon, M.-T. Th.; Lumbroso-Bader, N. *J. Am. Chem. Soc.* **1977**, *99*, 6838−6845. (d) Wagner, R.; von Philipsborn, W. *Helv. Chim. Acta* **1970**, *53*, 299−320. (e) Nguyen, V. Q.; Tureèek, F. *J. Am. Chem. Soc.* **1997**, *119*, 2280−2290. (f) Riand, J.; Coupry, C.; Chenon, M.-T. *J. Chem. Soc., Perkin Trans. 2* **1981**, 783−788. (g) Griffiths, D. V.; Swetnam, S. P. *J. Chem. Soc., Chem. Commun.* **1981**, 1224−1225.

(7) Demeter, Á.; Wéber, Cs.; Brlik, J. *J. Am. Chem. Soc.* **2003**, *125*, 2535−2540.

(8) Demeter, Á.; Wéber, Cs. *Concepts Magn. Reson., Part A* **2004**, *22* (1) 12−24.

(9) Gabriel, S.; Colman, J. *Chem. Ber.* **1899**, *32*, 1525−1538.

(10) (a) Gabriel, S. *Chem. Ber.* **1901**, *34*, 3362−3366. (b) Gerngross, O. *Chem. Ber.* **1905**, *38*, 3394−3408. (c) Wheland, R. S.; Martin, E. L. *J. Org. Chem.* **1975**, *40*, 3101−3109. (d) Mohrle, H.; Von der Lieck-Waldheim, *Sci. Pharm.* **1997**, *65* (3), 93−98. (e) Joshi, A. A.; Narkhede, S. S.; Viswanathan, C. L. *Bioorg. Med. Chem. Lett.* **2005**, *15*, 73−76.

(11) Hemmerich, P.; Prijs, B.; Erlenmeyer, H. *Helv. Chim. Acta.* **1959**, *42*, 1604−1611.

TABLE 1. ^{1}H NMR Chemical Shifts in ppm[a]

	H(5)	N(7)H_2 or N(7)(CH_3)$_2$	N(8,9)H_2 or N(8,9)(CH_3)$_2$	C(10)H_3	C(10)(CH_3)$_3$	others
1	4.86	5.49	5.58			
1N(1)	4.96	6.31	6.38			
2		5.24	5.51	1.69		
2N(1)		6.96	6.90	1.76		N(1,3)*H*, 10.44 br
3		5.06	5.15		1.36	
3N(1)		6.86	6.58		1.37	
3C(5)	3.08	8.31	*x* 8.64, *y* 8.85		0.98	
4	4.95	3.01	2.94			
4N(1)	5.17	3.13	3.08 br			N(1,3)*H*, 9.94 br
4C(5)	3.79	3.27	*x* 3.19, *y* 3.22			
5		3.01	2.83	1.91		
5C(5)	4.06 q	3.27	*x* 3.20, *y* 3.28	1.25 d		
7		*x* 3.11, *y* 3.16	*x* 2.78, *y* 3.04 *x* 3.30, 3.44 br			
7O		3.26	*x* 3.12, *y* 3.22 *x* 3.27, *y* 3.32			NO*H*, 14.37
8		3.12	3.09			
8C(5)	6.97	3.30	*x* 3.31, *y* 3.43			
9major		3.01	2.90			N*H*COCH$_3$, 8.54; NHCOC*H*$_3$, 1.90
9minor		3.03	2.94			N*H*COCH$_3$, 8.16; NHCOC*H*$_3$, 1.37
9C(5)	5.69 d	3.30	*x* 3.18, *y* 3.19			N*H*COCH$_3$, 9.00 d; NHCOC*H*$_3$, 1.88
10			5.15		1.37	Pyr-CH_2, 1.75−1.84 m; Pyr-NCH_2, 3.28−3.35 m
10C(5)	3.09		*x* 8.63, *y* 8.94		0.98	Pyr-CH_2, 1.80−2.00 m; Pyr-NC$H_{x,y}$, 3.42−3.56 m, 3.64−3.76 m
11			5.70		1.37	SCH_3, 2.32
11N(1)			7.00		1.36	SCH_3, 2.53; N(1,3)H, 12.52 br
11C(5)	3.27		*x* 9.72, *y* 9.97		0.97	SCH_3, 2.49

[a] The signals are singlets unless otherwise noted. d = doublet, q = quartet, m = multiplet, br = broad. *x*,*y* denotes peaks due to chemically nonequivalent Me groups or H atoms within a given NMe_2 or NH_2 group.

thus providing a convenient synthetic pathway to **5**. Under the same conditions, methylation of **1** gave only the N(1)-methylated product (see Supporting Information). The difference in the observed reactivity can be rationalized as follows. In **1**, the nucleophilic character of C(5) is weak compared to N(1), thus giving the N(1)-methylated derivative. In **4**, on the other hand, C(5) is a strong nucleophilic center leading to **5C(5)**. Because the N(1) position is sterically hindered by the bulky (dimethyl)-amino groups at C(2) and C(4,6), the less stable N(7)-methylated derivative is formed. *Tert*-butylation of **4** was attempted with *tert*-butyl-bromide and with the *tert*-butyl cation generated from isobutene, but formation of **6** could not be detected. HBF_4 salts of the respective bases were prepared by adding the acid in diethyl ether to the dichloromethane solution of the respective aminopyrimidine. **9** was synthesized from **7** in two steps. Catalytic hydrogenation of the nitroso compound **7** was followed by one-pot acylation of the 5-amino derivative with acetic anhydride.

NMR Spectroscopy. The increased electron density of the 2,4,6-triaminopyrimidine system, as compared to pyrimidine, becomes clearly visible by inspection of the respective chemical shifts (Tables 1−3). On the ^{15}N NMR spectra, the electron-donating resonance effect of the (dimethyl)amino groups results in a significant upfield shift of N(1,3) (Table 3) relative to pyrimidine.[6b] Moreover, a substantial upfield shift could be observed on the ^{13}C NMR spectra for C(5) (**1** $\Delta\delta$ −47.1 ppm, **4** $\Delta\delta$ −51.2 ppm, Table 2), which indicates increased electron density at this position as well. It is intriguing to investigate the effect of the alkyl substituents at C(5) on the NMR chemical shifts. We observed, in general, that substitution at C(5) results in a significant downfield shift of C(5) and a small downfield shift of N(1,3) (Tables 2 and 3), which points to decreased electron density at these atoms relative to the unsubstituted derivatives. We also observed an upfield shift at C(4,6) for **2** and **3**; however, in **5**, a significant downfield shift was detected. This can be rationalized intuitively; in **5**, the steric effect prevails over the electronic effect and indicates less conjugation of the (dimethyl)amino groups at C(4,6). The upfield shift of N(8,9) supports this assumption. These observations are in line with the calculated geometries and NPA charges (see below).

The base forms exhibit spectral symmetry with respect to the C(5)−C(2) axis except for **7**. In **7**, the conjugation of the electron-withdrawing nitroso group with the pyrimidine system is strong enough to cause slow NO rotation, i.e., slow mutual exchange on the NMR chemical shift time scale, which results in nonequivalence of the C(4) and C(6) as well as of the N(1) and N(3) atoms and also of the C(4)−NMe_2 and C(6)−NMe_2 groups. Moreover, the methyl groups within the (dimethyl)-amino groups at the C(2), C(4), and C(6) atoms also show chemical shift nonequivalence due to the double bond character of the *C*-*N*Me_2 bonds. Rotation of the (dimethyl)amino groups for the other investigated bases is fast on the NMR chemical shift time scale. In the ^{1}H, ^{13}C, and ^{15}N NMR spectra of **9**, two signal sets were observed due to the cis and trans amide rotamers. On the basis of the measured strong N*H*−COC*H*$_3$ NOE, we assign the major species (80%) to the trans amide rotamer.

NMR investigations of the respective HBF_4 salts expose the protonation behavior of the studied compounds. Because of the relatively large activation energy associated with carbon protonation of aromatic systems (i.e., sigma complex formation), C(5) protonation is a slow process. Therefore, the exchange between C(5) and N(1) protonated forms is slow on the NMR chemical shift time scale and separate signals are observed. Integration of the equilibrium intensities gives the population ratio indicative of the thermodynamic stability of the carbon

TABLE 2. ^{13}C NMR Chemical Shifts in ppm[a]

	C(2)	*C*(4)	*C*(6)	*C*(5)	N(7)(*C*H$_3$)$_2$	N(8,9)(*C*H$_3$)$_2$	*C*(10)H$_3$	*C*(10)(CH$_3$)$_3$	C(10)(*C*H$_3$)$_3$	others
1	163.1	164.5		74.8						
1N(1)	157.7	161.6		73.7						
2	160.6	162.2		80.2			9.0			
2N(1)	152.4	157.7		79.3			8.2			
3	159.2	162.0		93.5				32.1	31.3	
3C(5)	167.4	172.3		48.9				36.9	27.7	
4	160.9	163.7		70.7	36.2	36.6				
4N(1)	152.5	161.6	154.7	71.7	37.7	38.7 br, 37.6 br				
4C(5)	163.0	166.5		25.3	37.0	37.7				
5	158.5	167.7		87.2	36.2	40.3	16.2			
5C(5)	162.0	170.9		28.2	37.0	*x* 37.9, *y* 37.8	17.0			
7	158.9	152.5	164.8	140.1	*x* 36.5, *y* 36.6	*x* 41.5, *y* 36.7 br *x* 37.8, *y* 42.4 br				
7O	159.1	156.5	160.2	137.9	*x* 37.5, *y* 37.6	*x* 41.8, *y* 37.3 *x* 38.1, *y* 41.0				
8	158.5	160.7		104.1	36.6	39.8				
8C(5)	160.6	158.2		69.7	37.6	*x* 39.1, *y* 39.3				
9major	158.0	163.8		90.4	36.3	40.0				*C*OCH$_3$, 168.1; COC*H*$_3$, 22.2
9minor	158.1	163.7		92.4	36.3	40.0				*C*OCH$_3$, 172.4; COC*H*$_3$, 19.5
9C(5)	161.3	165.8		37.2	37.3	*x* 38.3, *y* 38.3				*C*OCH$_3$, 168.7; COC*H*$_3$, 21.9
10	157.1	161.6		92.8				32.0	31.3	Pyr-*C*H$_2$, 25.0; Pyr-NCH$_2$, 45.7
10C(5)	162.3	171.3		49.1				36.5	27.6	Pyr-*C*H$_2$, 24.4; Pyr-NCH$_2$, 47.5
11	163.7	161.1		97.2				32.2	30.5	S*C*H$_3$, 12.8
11N(1)	157.8	157.0 br		95.7				32.3	29.6	S*C*H$_3$, 12.8
11C(5)	189.1	172.9		49.9				38.1	27.5	S*C*H$_3$, 13.9

[a] br = broad. *x*,*y* denotes peaks due to chemically nonequivalent Me groups within a given NMe$_2$ group.

TABLE 3. ^{15}N NMR Chemical Shifts in ppm[a]

	N(1)	*N*(3)	*N*(7)	*N*(8,9)	others
1	−190		−305	−307	
1N(1)	−213		−305	−302	
2	−188		−306	−306	
2N(1)	−228		−303	−297	
3	−182		−308	−300	
3C(5)	−184		−268	−257	
4	−193		−317	−319	
4N(1)	−299	−198	−307	−313	
4C(5)	nd		−276	−268	
5	−178		−317	−324	
5C(5)	−195		−277	−268	
7	−192	−189	−294	−279, −289	*N*O, nd
7O	−182	−183	−273	−262, −271	*N*OH, 23
8	−185		−296	−280	*N*O$_2$, −27
8C(5)	−193		−271	−260	*N*O$_2$, −16
9major	−182		−317	−322	*N*HCOCH$_3$, −263
9minor	−183		−315	−321	*N*HCOCH$_3$, −262
9C(5)	−191		−275	−268	*N*HCOCH$_3$, −265
10	−183		−295	−300	
10C(5)	−185		−251	−258	
11	−155			−296	
11N(1)	nd			−288	
11C(5)	−168			−243	

[a] nd = not detected.

and the nitrogen protonated species (Table 7, see below). Reaching thermal equilibrium was generally fast (from a few minutes to hours at 30 °C), and it was further checked after several weeks. In the case of **3**, we observed a somewhat slower process. The first major species **3N(1)** (kinetically controlled form) was gradually transformed to the thermodynamically more stable **3C(5)** form, attaining the equilibrium after a few weeks at room temperature.

It has been found that **5**, **9**, and **10** are fully C(5) protonated, that **1** and **2** are fully N(1) protonated, and that **3**, **4**, and **11** exhibit equilibrium between both forms under the applied experimental conditions (Table 7, see below). The C(5)H/N(1)H population ratio can be fine tuned with the appropriate substituent. The stronger and weaker electron-donating pyrrolidine and SMe groups at C(2) in **10** and **11** can increase or decrease the relative amount of the C(5) protonated form relative to **3**, indicating a strong electronic substituent effect. It is interesting to note that **7** protonates fully at the nitroso oxygen. We observed that the HBF_4 salt of **8** was not stable in DMSO-d_6. In a freshly prepared solution, the presence of **8C(5)** (7%) could be detected together with the base form **8**. The solution slowly transforms to the HBF_4 salt of **4**, which can be rationalized by elimination of NO_2^+ from the intermediate **8C(5)**. Because NO_2 is a good leaving group, the elimination is favored in this case, and the σ-complex was of only transitory existence.

The C(5) protonated forms give characteristic NMR spectra. The H(5) proton appears as a sharp singlet for **3C(5)**, **4C(5)**, **8C(5)**, **10C(5)**, and **11C(5)**, whereas it shows up as a quartet for **5C(5)** (^3J = 7.4 Hz) and as a doublet for **9C(5)** (^3J = 9.2 Hz) due to the C(5)*H*−C*H*$_3$ and C(5)*H*−N*H*COCH$_3$ vicinal couplings, respectively. The C(5) carbon experiences a substantial upfield shift (e.g., 45 and 59 ppm for **4** and **5**) relative to the base form as a result of the sp^2 to sp^3 hybridization change (Table 2). ^{13}C and ^{15}N chemical shift changes indicate effective delocalization of the positive charge on the σ-complex frame: C(2), C(4), and C(6) show characteristic downfield shifts in line with their positively charged character (Table 2). Similarly, ^{15}N chemical shifts of N(7) and N(8,9) experience substantial downfield shifts, and N(1,3) shows a small, but characteristic, upfield shift (Table 3) with respect to the base forms. The observed chemical shift changes are in line with the calculated NPA charges and the alternating charge distribution (see below). It is interesting to note that in the C(5) protonated form the substituents at C(5) assume a quasiaxial orientation (Figure 1b), whereas in the base form they are aligned with the pyrimidine ring plane. This geometrical change gives rise to the observed

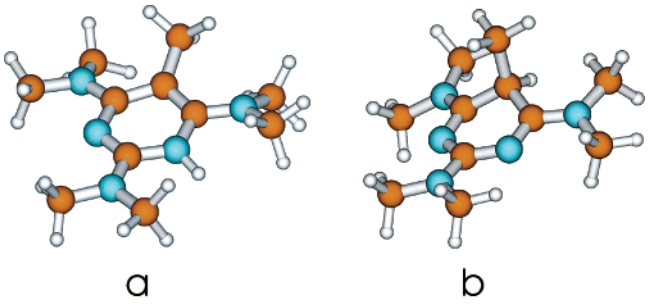

FIGURE 1. Optimized geometry of (a) **5N(1)** and (b) **5C(5)** using B3LYP/cc-pVDZ.

CHART 3

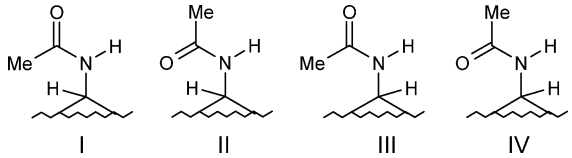

upfield shift of the ^{1}H signals due to the Me and *t*Bu groups in **3**, **5**, **10**, and **11** (Table 1) relative to the respective base because these protons experience the anisotropic shielding and deshielding effects of the pyrimidine ring in the C(5) protonated and base forms, respectively. In line with our previous observations,[7] rotation of the N(8,9) (dimethyl)amino groups in the studied σ-complexes is slow on the NMR chemical shift time scale and separate ^{1}H and ^{13}C signals are detected. The assignment of the signals due to the chemically nonequivalent H atoms or Me groups within NH_2 or NMe_2 groups is based on the measured C(5)*H*−N(8,9)*Me*$_x$ NOE. Accordingly, the upfield H$_x$ atom or Me$_x$ group is close in space to C(5)*H* (see Tables 1 and 2). The double bond character indicates that conjugation of the (dimethyl)amino groups stabilizes the positively charged σ-complex. Carbon protonation of **9** gives rise to four possible conformers as shown in Chart 3.

However, only one signal set was observed indicating either slow exchange with a single predominant conformation or fast equilibrium between these forms on the NMR chemical shift time scale. The observed strong N*H*−COC*H*$_3$ NOE and the lack of dipolar interaction between C(5)*H* and COC*H*$_3$ point to a trans amide bond (form II and IV). On the basis of the measured relatively large C(5)*H*−N*H*COCH$_3$ vicinal coupling (^3J = 9.2 Hz) and the observed strong C(5)*H* and N*H*COCH$_3$ NOE, we conclude that under the given conditions form IV is the predominant conformer with a coplanar arrangement of the C(5)-*H* and N*H*COCH$_3$ protons according to the calculated geometry of conformer IV (see Supporting Information).

The N(1) protonated form is characteristic of the observed upfield shifts of C(2), C(4,6), and N(1,3) and the downfield shift of N(7) and N(8,9) as well as of N(7)*H*$_2$/(C*H*$_3$)$_2$ and N(8,9)-*H*$_2$/(C*H*$_3$)$_2$ relative to the base (Tables 1−3). In the case of **1N-(1)**, **2N(1)** and **11N(1)**, the mutual exchange between the N(1) and N(3) protonated forms is fast on the NMR chemical shift time scale and apparent spectral symmetry with respect to the C(5)−C(2) axis is observed due to signal averaging. In the case of **1N(1)**, the N(1)*H* signal is broadened to the extent that it escapes detection; on the other hand, the N(1)*H* signal of **2N-(1)** and **11N(1)** are observable as a broad singlet signal. For **4N(1)**, however, the exchange is slow on the ^{13}C and ^{15}N chemical shift time scale and separate signals are observed for the N(1) and N(3), C(4) and C(6), and N(7)(C*H*$_3$)$_2$ and N(8)-(C*H*$_3$)$_2$ pairs. The slower exchange in **4N(1)** can be attributed to the steric hindrance of the N(1) and N(3) positions due to the bulky (dimethyl)amino groups.

It is also interesting to discuss the oxygen protonation of **7**. In the base, conjugation of the nitroso group with the pyrimidine system is strong resulting in the partial double bond character of the C(5)−NO bond. This shows up in the relatively large (ca. 140 ppm) chemical shift of C(5) relative to **4**. Upon protonation at the nitroso oxygen, the resulting system can be described with the C(5)═N−OH oxime-type bond and the delocalization of the positive charge in the pyrimidine ring similar to that observed for the C(5) protonated forms. Similar to the base form (**7**), **7O** is asymmetrical with respect to the C(5)−C(2) axis, and rotation of the (dimethyl)amino groups is a slow process as indicated by the observed chemical shift nonequivalence of the methyl signals.

Computational Results. All the calculated geometrical data are summarized in the Supporting Information. Geometry optimization of the base forms using the B3LYP/cc-pVDZ method showed that fully planar rings with coplanar amino or (dimethyl)amino groups do not present local minima on the potential energy surface (PES), and the exocyclic nitrogens are slightly pyramidal. The pyramidal nitrogens allow various conformers with different orientation of the (dimethyl)amino groups. However, it was found that the PES is shallow and the calculated conformers are energetically very close to each other. Therefore, in our study, we selected and compared the same conformer of all the compounds. In this conformer, the lone pairs of exocyclic **8** and **9** nitrogens are on the same side of the ring plane. The nearly planar arrangement of the (dimethyl)-amino groups indicates substantial conjugation with the pyrimidine ring. In the case of **9**, the four possible conformers were also studied. The steric effect of the C(5) substituents hampers full delocalization, hence it causes a slight shift of the C(5) atom out of the ring plane and a small twist of the (dimethyl)amino groups at C(4) and C(6) with respect to the ring plane (Figure 1). The steric effect increases in the order of **1** < **2** < **3** and **4** < **5** < **6** and is stronger in the (dimethyl)amino series (**4**−**6**).

While in the N(1) protonated derivatives, the geometries of the (dimethyl)amino groups are similar to the base forms (Figure 1a), protonation at C(5) results in a planar structure of the frame, with the exception of the C(5) atom (Figure 1b). In the C(5) protonated forms, conjugation of the C(4,6) (dimethyl)amino group is stronger compared to the base forms which could explain the observed stability of the σ-complex.

The differences in geometry and also natural population analysis (NPA)[12] charges between gas-phase and solvated-phase structures are negligible (see Supporting Information). As expected, the ring and exocyclic nitrogen atoms are highly negative. However, it was found that the charge on C(5) is also strongly negative in all bases which can be explained by the electron-donating effects of different substituents. Earlier calculations suggested that the negative charge on C(5) in the pyrimidine ring undergoes monotonic increases while connecting more amino substituents.[13] We found that the charge in substituted 2,4,6-triaminopyrimidines is competitive with that of N(1,3) which rationalizes the protonation at C(5). In our study, protonation was theoretically examined at each of the six negative centers of the framework (Table 4).

(12) Reed, A. E.; Weinstock, R. B.; Weinhold, F. *J. Chem. Phys.* **1985**, *83*, 735−746.
(13) Barfield, M.; Fagerness, P. *J. Am. Chem. Soc.* **1997**, *119*, 8699−8711.

TABLE 4. NPA Charges of 1 and Its Protonated Derivatives[a]

	1	1C(5)	1N(1)	1N(7)	1N(8)
N(1)	−0.657	−0.630	−0.636	−0.618	−0.606
C(2)	0.691	0.730	0.736	0.649	0.701
N(3)	−0.657	−0.630	−0.615	−0.619	−0.632
C(4)	0.487	0.578	0.517	0.491	0.419
C(5)	−0.459	−0.586	−0.427	−0.404	−0.424
C(6)	0.487	0.578	0.509	0.490	0.515
N(7)	−0.821	−0.724	−0.796	−0.771	−0.781
N(8)	−0.818	−0.752	−0.758	−0.780	−0.764
N(9)	−0.818	−0.752	−0.794	−0.780	−0.776
H(10)	0.222	0.292	0.259	0.251	0.252
H^+		0.292	0.431	0.470	0.462

[a] NPA charges were calculated at the B3LYP/cc-pVDZ level in the gas phase.

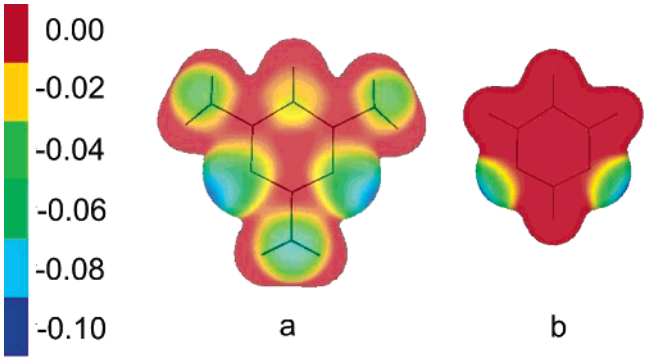

FIGURE 2. Molecular electrostatic potential of (a) **1** and (b) pyrimidine. The MEP values are plotted on a 0.01 electron density value, calculated by the polarized continuum model (PCM; DMSO solution) with B3LYP/cc-pVDZ.

In the carbon protonated forms, the charge on C(5) decreases which confirms the appearance of a new delocalization in these structures because the positive charge is shared in the molecular frame. This can be seen on the charges of the exocyclic nitrogen atoms; hence their growth is around 0.07−0.1. On the other hand, if a nitrogen atom is protonated, the conjugation of the positive charge is less effective. This can also be obtained from the calculated nucleus-independent chemical shifts (NICS)[14] (see Supporting Information). In comparison, for pyrimidine, all base forms which have an electron-donating substituent at C(5) are less aromatic (−7.02 (pyrimidine) changes between −4 and −6) and the aromaticity decreases with the N(1) protonation. Electron-withdrawing substituents in **7** and **8** highly decrease NICS values to −2.22 and −3.36, respectively. All carbon protonated forms and **7O** have positive NICS indices which indicate that the aromatic system indeed ceases.

The charge distribution was also investigated with molecular electrostatic potential (MEP),[15] mapped on an isoelectron density surface for all the studied molecules. Figure 2 shows the results for **1** and, as a comparison, for pyrimidine. All the other MEPs are in the Supporting Information.

A previous study showed that protonation at the C(5) position is not predictable by the MEP of nonsubstituted pyrimidine.[16] Our calculations show that in the substituted derivatives C(5) has a strongly negative MEP value and all the other nucleophilic centers in the frame are in nitrogen atoms. In all molecules, the MEP values indicate more negative nitrogens than C(5) which suggests that N(1) protonation is favorable under kinetic control. As a conclusion, when C(5) protonation is favored, it should be under thermodynamical control. This phenomenon was clearly observed by NMR spectroscopy and discussed in the NMR section. Note that the MEP values in DMSO are normally smaller than those in the gas phase, although the tendency of the charge distribution is the same in both phases.

TABLE 5. Calculated Proton Affinities[a]

	C(5)	N(1)	N(7)	N(8)	O
1	990.1	1005.2	928.1	910.2	
2	988.0	1010.0	934.3	917.8	
3	1033.6	1012.1	936.2	927.5	
4	1034.4	1034.6	985.4	966.9	
5	1058.0	1030.4	976.5	977.2	
6	1110.6	1033.1	975.0	992.6	
7	982.1	993.2	940.7	948.2	1048.4
8	1006.4	983.6	933.4	942.5	989.0
9	1056.4	1025.0			965.9
10	1056.7	1031.1	980.8	944.5	
11	996.1	1007.2		910.6	

[a] The B3LYP/cc-pVDZ method was used. The values are in kJ/mol and belong to the most stable studied conformers (see Supporting Information). The PA of **7N(10)** is 1011.4 kJ/mol.

The gas-phase proton affinity (PA) has been calculated for the following reaction:[17]

$$B + H^+ \rightleftarrows BH^+$$

where B is the base form and BH^+ is the protonated form. The PAs were calculated using eq 1:

$$PA = -\Delta H = \Delta E_{tot} + \Delta ZPE + \frac{5}{2}RT \qquad (1)$$

where ΔH is the enthalpy change of the protonation reaction, E_{tot} is the electron energy at 0 K, ZPE is the zero point correction, R is the molar gas constant, and T is the absolute temperature in kelvin.

The results show that in the studied molecules the PA of C(5) and N(1) is commensurable, and the protonation of exocyclic nitrogens is not favored (Table 5).

1N(1) is the most stable of the protonated forms of **1**. The electron-donating effect of the methyl group slightly raises the PA at N(1), N(7), and N(8) but not at C(5); therefore, in the case of **2**, carbon protonation is not expected. In **3**, because of the bulky *tert*-butyl group, the steric effect of the C(5) substituent can appear as a relevant factor and causes the highest PA at C(5). In the cases of **4**−**6**, the tendency is almost the same as that in **1**−**3**, but changing the amino groups to (dimethyl)amino groups raises the PAs and the relevance of the steric effects. By comparing **7** and **8** with other studied molecules, it can be seen that the electron-withdrawing groups decrease the PA at all positions. In both cases, oxygen protonation was also studied and we found that in **7** this site has the highest PA. It can be concluded that C(5) protonation is favorable with large and electron-donating substituents. Therefore, it is expected that the bulky acetamino substituent causes high PA at the C(5) position in **9**. The PA at the N(1)/C(5) position can be fine tuned not only by C(5) but also by

(14) Schleyer, P. v. R.; Maerker, C.; Dransfeld, A.; Jiao, H.; Hommes, N. J. R. v. E. *J. Am. Chem. Soc.* **1996**, *118*, 6317−6318.

(15) Náray-Szabó, G.; Ferenczy, Gy. G. *Chem. Rev.* **1995**, *95*, 829−847.

(16) Shukla, M. K.; Mishra, P. C. *J. Chem. Inf. Comput. Sci.* **1998**, *38*, 678−684.

(17) Szulejko, J. E.; McMahon, T. B. *J. Am. Chem. Soc.* **1993**, *115*, 7839−7848.

TABLE 6. Calculated Relative Gibbs Free Energies (in DMSO) and Relative PAs[a]

	ΔG[b]					ΔPA[c]				
	C(5)	N(1)	N(7)	N(8)	O	C(5)	N(1)	N(7)	N(8)	O
1	18.7	0.0	74.4	84.6		15.1	0.0	77.1	95.0	
2	31.3	0.0	77.6	88.0		22.0	0.0	75.6	92.2	
3	0.0	2.4	79.1	96.0		0.0	21.5	97.4	106.1	
4	0.0	1.9	62.5	70.4		0.2	0.0	49.2	67.7	
5	0.0	27.6	85.3	69.0		0.0	27.7	81.5	80.8	
6	0.0	64.2	123.6	107.2		0.0	77.6	135.7	118.0	
7	54.0	36.0	87.9	82.3	0.0	66.3	55.3	107.7	100.3	0.0
8	0.0	13.2	56.7	54.8	22.4	0.0	22.8	73.0	63.9	17.4
9	0.0	24.7				0.0	31.4			90.5
10	0.0	19.5	83.3	90.4		0.0	25.6	75.9	112.3	
11	17.0	0.0		77.6		11.0	0.0		96.6	

[a] Values are in kJ/mol and belong to the most stable studied conformers (see Supporting Information). [b] The PCM method was used at the B3LYP/cc-pVDZ level. [c] The B3LYP/cc-pVDZ level in the gas phase.

TABLE 7. Experimental and Calculated Boltzmann Distributions

	calculated distribution[a]			measured distribution[b]		
	C(5)	N(1)	O	C(5)	N(1)	O
1	0	100		nd	100	
2	0	100		nd	100	
3	71	29		96	4	
4	68	32		10	90	
5	100	0		100	nd	
6	100	0				
7[c]	0	0	100	nd	nd	100
8	100	0	0	d	nd	
9	100	0		100	nd	
10	100	0		100	nd	
11	0	100		9	91	

[a] Values are in %. The PCM method was used at the B3LYP/cc-pVDZ level. The values belong to the most stable studied conformers (see Supporting Information). [b] Values measured by NMR in DMSO-d_6 with integration of the respective forms. nd = not detected. d = detected. [c] The calculated Boltzmann distribution of **7N(10)** is 0.0%.

C(2) substitution, as **3**, **10**, and **11** show. The electron donation of C(2) substituents raises the PA in the order of **11** < **3** < **10**. This effect is larger at C(5) than at N(1); as a consequence, in **10**, the C(5) protonation overrides N(1). The high PA at C(5) in the crowded C(5) substituted molecules suggests that the stability effect of new delocalization and the termination of the steric strain are comparable with the stabilization effect of the aromatic system.

Considering the Boltzmann distribution, the population ratio of the different protonated forms can be calculated as follows:

$$\frac{N(BH_1^+)}{N(BH_2^+)} = \exp\left[-\frac{\Delta G_{12}}{RT}\right] \qquad (2)$$

where $N(BH_1^+)$ and $N(BH_2^+)$ are the populations of the two protonated forms and ΔG_{12} is the Gibbs free energy difference. ΔG_{12} was calculated using the PCM method which includes solvation effects. The calculated distribution can be directly compared with the protonation distribution measured by NMR.

In Table 6 the relative energy values in the gas phase and in DMSO solution are compared. The correlation between ΔG in DMSO and ΔPA is linear with 0.96 R^2 (Chart SI 1, see Supporting Information), which shows that the gas-phase calculations simulate the protonation site well.

The experimental and calculated Boltzmann distributions are given in Table 7. Because of the exponential function, the calculated Boltzmann distribution is very sensitive to slight energy differences. Considering the inherent calculation errors, the applied model reproduces the experimental protonation well. If, however, there are two energetically close forms, a precise population ratio cannot be predicted.

Conclusions

The protonation of a series of different C(5) substituted 2,4,6-triaminopyrimidine derivatives was investigated. For this purpose, we synthesized several new 2,4-diamino- and 2,4,6-triaminopyrimidines and their respective HBF_4 salts. The site of the protonation was studied experimentally by ^{1}H, ^{13}C, and ^{15}N NMR spectroscopy and theoretically by using PCM B3LYP/cc-pVDZ quantum chemical methods. Generally, protonation sites were found at the C(5) and N(1) positions. The C(5)H/N(1)H population ratio strongly depends on the substituents present. The results of the quantum chemical calculations are in accord with the experimental observations and prove that combined steric and electronic effects are responsible for the observed C(5) protonation and for σ-complex stability. The steric clash between the nearly coplanar substituents at C(5) and at C(4,6) in the base is partly relieved in the σ-complex, where the C(5) substituent assumes quasiaxial orientation perpendicular to the ring plane. This gives rise to stronger conjugation of the (dimethyl)amino substituents at C(4,6) relative to the base, leading to electronic stabilization of the σ-complex through an effective charge delocalization. Our results prove that C(5) protonation is a general feature of the 2,4,6-triaminopyrimidine system. The observed carbon protonation receives attention in connection with structure−activity relationship studies of pharmaceutically active compounds containing the 2,4,6-triaminopyrimidine moiety.

Experimental Section

The general spectroscopic and computational methods are given in the Supporting Information.

Synthetic Methods. 5-*tert*-Butyl-2,4,6-triaminopyrimidine (3). Sodium *tert*-butylate (0.42 g, 4.37 mmol) was dissolved in abs ethanol (2 mL). Guanidine hydrochloride (0.36 g, 3.77 mmol) and *tert*-butylmalonitrile[10c] (0.5 g, 4.1 mmol) were added, and the reaction mixture was stirred for 2 h at 90 °C under reflux. The solvent was evaporated in a vacuum. The residue was stirred with water (3 mL), and the resultant solid was filtered off, washed with water (2 × 1 mL), stirred with diethyl ether (5 mL), and filtered off again to give **3** as a yellowish solid. Yield 67%. Mp 232−233 °C. IR (KBr, cm^{-1}): ν = 3518, 3467, 3393, 3349, 3177, 2956, 1662, 1635, 1565, 1406, 1037, 804. HRMS *m*/*z* calcd for $C_8H_{15}N_5$, 181.1322; found, 181.1319.

5-Methyl-2,4,6-tris(dimethylamino)pyrimidine (5). Iodomethane (1.55 mL, 25 mmol) was added to a solution of 2,4,6-tris-(dimethylamino)pyrimidine (1.04 g, 5 mmol) in dichloromethane (5 mL). The solution was refluxed for 120 h at 40 °C, and then the solvent was removed in a vacuum to give a crude product, which contained two main components (TLC/ethyl acetate/MeOH/25% NH_3 solution in water = 10:0.1:0.01). The two components of the crude product were separated by silica gel gradient flash chromatography (eluent A: ethyl acetate/MeOH/25% NH_3 solution in water = 10:0.1:0.01; eluent B: ethyl acetate/MeOH/25% NH_3 solution in water = 10:3:0.1) to give 475 and 878 mg of product, respectively. These products were dissolved in dichloromethane (10 mL), and the solutions were extracted with 20 m/m% sodium carbonate solution in water (2 × 10 mL) and dried over anhydrous sodium sulfate. The drying agent was filtered off, and the solvents were evaporated in a vacuum to give 284 and 521 mg of methylated

pyrimidine derivative, respectively. The major product (N(7)-methylated derivative) was obtained as a semisolid. It proved to be unstable, and it was not characterized in detail. Its structure was confirmed by NMR (see Supporting Information). On the basis of NMR, the minor product proved to be the 5-methyl-2,4,6-tris-(dimethylamino)pyrimidine (**5**). Yield: 25.3%. Mp 97−98 °C. IR (KBr, cm^{-1}): ν = 3429, 2945, 2861, 1565, 1383, 1140, 1070, 1032, 795. HRMS *m*/*z* calcd for $C_{11}H_{21}N_5$, 223.1791; found, 223.1797.

2,4,6-Tris(dimethylamino)-5-nitrosopyrimidine (7). 2,4,6-Tris-(dimethylamino)pyrimidine (1.5 g, 7.17 mmol) was dissolved in a mixture of dichloromethane (12 mL) and acetic acid (2.5 mL). A solution of $NaNO_2$ (0.7 g, 14 mmol) in water (5 mL) was added dropwise at 0−5 °C over a period of 15 min, and then the resultant mixture was stirred for 1 h at the same temperature. The reaction mixture was diluted with water (25 mL) and dichloromethane (25 mL) followed by basifying the solution to pH 10 with sodium carbonate. The organic layer was separated and dried over anhydrous sodium sulfate, and the solvent was evaporated to give **7**. The crude product was purified by silica gel column chromatography (100 g of silica gel, $CHCl_3$/MeOH = 99:1) to give 1.28 g of product as a blue solid. Yield: 75%. Mp 191−192 °C. IR (KBr, cm^{-1}): ν = 2924, 1510, 1555, 1398, 1247, 1071, 778. HRMS *m*/*z* calcd for $C_{10}H_{18}N_6O$, 238.1537; found, 238.1544.

5-Nitro-2,4,6-tris(dimethylamino)pyrimidine (8). 2,4,6-Tris-(dimethylamino)pyrimidine (500 mg, 2.39 mmol) was dissolved in dichloromethane (5.0 mL). The solution was cooled to −70 °C under an argon atmosphere, and solid nitronium tetrafluoroborate diethyl etherate (740 mg, 5.52 mmol) was added in five portions over a period of 2 h. The resultant mixture was stirred at −70 °C for 4 h, allowed to warm, and then stirred for 24 h at room temperature. Dichloromethane (15 mL) was added, and the resultant solution was extracted with a solution of sodium carbonate (c = 20 m/m%, 3 × 5 mL). The organic layer was dried over anhydrous sodium sulfate and filtered, and the solvent was removed in a vacuum to give a crude product (520 mg), which was purified by gradient flash chromatography (40 g of silica gel; eluent A: *n*-hexane; eluent B: ethyl acetate). Yield: 35%. Description: white solid. Mp 209−210 °C. IR (KBr, cm^{-1}): ν = 2931, 1558, 1477, 1396, 1312, 1277, 1057, 777, 722. HRMS *m*/*z* calcd for $C_{10}H_{18}N_6O_2$, 254.1486; found, 254.1479.

5-Acetylamino-2,4,6-tris(dimethylamino)pyrimidine (9). 5-Nitroso-2,4,6-tris(dimethylamino)pyrimidine (**7**, 0.92 g, 3.86 mmol) was dissolved in a mixture of tetrahydrofuran (100 mL) and acetic anhydride (1.2 mL, 11.1 mmol). Palladium on carbon (0.2 g, loading: 10 m/m%) was added, and hydrogen was bubbled through the solution for 3 h. The catalyst was filtered off and washed with methanol, and the resultant solution was concentrated in a vacuum. The residue was stirred with ethanol, and the solid was filtered off and washed with ethanol and diethyl ether to give **9** as a white solid. Yield: 32%. Mp 213−214 °C. IR (KBr, cm^{-1}): ν = 3295, 2940, 2874, 1660, 1559, 1506, 1281, 1053, 783. MS *m*/*z* calcd for $C_{12}H_{22}N_6O$, 266.1850; found, 266.1844.

5-*tert*-Butyl-4,6-diamino-2-(pyrrolidin-1-yl)pyrimidine (10). Sodium *tert*-butylate (1.26 g, 13 mmol) was dissolved in abs ethanol (12 mL). *tert*-Butylmalonitrile[10c] (2.0 g, 12.3 mmol) and pyrrolidine-1-carboxamidine hydrogen sulfate[18] (1.5 g, 13 mmol) were added, and the mixture was stirred for 8 h at 90 °C under reflux. The solvent was removed in a vacuum, and water (15 mL) was added. The mixture was stirred for 2 h at room temperature. The solid was filtered off, washed with water, and recrystallized from boiling ethanol to give **10** as a white solid. Yield: 64%. Mp 222−223 °C. IR (KBr, cm^{-1}): ν = 3543, 3282, 3153, 2948, 2853, 1617, 1539, 1346, 1185, 796. HRMS *m*/*z* calcd for $C_{12}H_{21}N_5$, 235.1791; found, 235.1791.

5-*tert*-Butyl-4,6-diamino-2-methylsulfanylpyrimidine (11). Sodium *tert*-butylate (0.38 g, 3.96 mmol) was dissolved in abs ethanol (2 mL). *tert*-Butylmalonitrile[10c] (0.5 g, 4.1 mmol) and thiocarbamide (0.3 g, 3.95 mmol) were added, and the mixture was stirred for 5 h at 90 °C under reflux. The solvent was removed in a vacuum, and water (2 mL) and a solution of hydrochloric acid (0.87 mL, c = 16 m/m%, 4.1 mmol HCl) were added dropwise. The mixture was stirred for 2 h at room temperature. The solid was filtered off and washed with water to give 5-*tert*-butyl-4,6-diamino-2-thiopyrimidine (0.38 g, yield: 47%), which was used without further purification for preparation of **11**.

Sodium *tert*-butylate (0.20 g, 2.08 mmol) was dissolved in abs ethanol (3.5 mL). 5-*tert*-Butyl-4,6-diamino-2-thiopyrimidine (0.35 g, 1.77 mmol) and iodomethane (0.115 mL, 1.85 mmol) were added, and the mixture was stirred at room temperature for 2 h. The solvent was evaporated in a vacuum. The residue was dissolved in dichloromethane (5 mL), and the dichloromethane solution was extracted with water (3×5 mL) and dried over anhydrous sodium sulfate. The drying agent was filtered off, and the solvent was removed in a vacuum to give a crude product, which was recrystallized from ethanol. Yield: 64% (referring to 2-thiopyrimidine derivative), 30% (referring to *tert*-butylmalonitrile). Description: white solid. Mp 180−181 °C. IR (KBr, cm^{-1}): ν = 3538, 3417, 3302, 3172, 2954, 2875, 1631, 1596, 1536, 1436, 1398, 1308, 956, 759. HRMS *m*/*z* calcd for $C_9H_{16}N_4S$, 212.1090; found, 212.1079.

General Procedure for the Preparation of the HBF_4 Salts of Compounds 1−11. The aminopyrimidine derivative (2 mmol) was dissolved in methanol (5.0 mL) at room temperature. The solution was cooled to 0 °C under an argon atmosphere, and then a solution of tetrafluoroboric acid diethyl etherate in diethyl ether (2.1 mL, c = 1 M) was added dropwise over a period of 5 min. The solvent was removed in a vacuum, and the residue was stirred with diethyl ether (3 mL). The solid was filtered off, washed with diethyl ether, and dried in a vacuum to give the HBF_4 salt of the aminopyrimidine.

5-Methyl-2,4,6-triaminopyrimidinium Tetrafluoroborate (2·HBF_4). Yield: 87%. Mp 245−246 °C. Description: white solid. IR (KBr, cm^{-1}): ν = 3474, 3147, 3389, 3210, 2945, 1638, 1452, 1367, 1054 (BF_4^-), 708. HRMS *m*/*z* calcd for $C_5H_9N_5$, 139.0852; found, 139.0853.

5-*tert*-Butyl-2,4,6-triaminopyrimidinium Tetrafluoroborate (3·HBF_4). Yield: 89%. Mp 209−210 °C. Description: white solid. IR (KBr, cm^{-1}): ν = 3549, 3533, 3458, 3406, 3209, 2969, 1681, 1630, 1435, 1360, 1100 and 1056 (BF_4^-), 993, 776. HRMS *m*/*z* calcd for $C_8H_{15}N_5$, 181.1322; found, 181.1336.

2,4,6-Tris(dimethylamino)pyrimidinium Tetrafluoroborate (4·HBF_4). Yield: 84%. Mp 243−245 °C. Description: white solid. IR (KBr, cm^{-1}): ν = 3418, 2949, 1632, 1583, 1412, 1334, 1175, 1057 (BF_4^-), 766. HRMS *m*/*z* calcd for $C_{10}H_{19}N_5$, 209.1635; found, 209.1621.

2,4,6-Tris(dimethylamino)-5-methylpyrimidinium Tetrafluoroborate (5·HBF_4). Yield: 78%. Mp 177−178 °C. Description: white solid. IR (KBr, cm^{-1}): ν = 3400, 2946, 2770, 1594, 1393, 1054 (BF_4^-), 756. HRMS *m*/*z* calcd for $C_{11}H_{21}N_5$, 223.1791; found, 223.1786.

2,4,6-Tris(dimethylamino)-5-nitrosopyrimidinium Tetrafluoroborate (7·HBF_4). Yield: 81%. Mp 196−197 °C. Description: blue solid. IR (KBr, cm^{-1}): ν = 3324, 2941, 1649, 1578, 1372, 1075 (BF_4^-), 1005, 764. HRMS *m*/*z* calcd for $C_{10}H_{18}N_6O$, 238.1537; found, 238.1535.

5-Acetylamino-2,4,6-tris(dimethylamino)pyrimidinium Tetrafluoroborate (9·HBF_4). Yield: 92%. Mp 244−246 °C. Description: white solid. IR (KBr, cm^{-1}): ν = 3379, 2953, 1692, 1530, 1594, 1390, 1291, 1069 (BF_4^-), 788. HRMS *m*/*z* calcd for $C_{12}H_{22}N_6O$, 266.1850; found, 266.1851.

5-*tert*-Butyl-4,6-diamino-2-(pyrrolidin-1-yl)pyrimidinium Terafluoroborate (10·HBF_4). Yield: 91%. Mp 241 °C. Description: white solid. IR (KBr, cm^{-1}): ν = 3368, 3180, 2973, 1670, 1586, 1364, 1057 (BF_4^-), 999, 753. HRMS *m*/*z* calcd for $C_{12}H_{21}N_5$, 235.1791; found, 235.1797.

(18) Bannard, R. A. B.; Casselman, A. A.; Cockburn, W. F.; Brown, G. M. *Can. J. Chem.* **1958**, *36*, 1541−1549.

5-*tert*-Butyl-4,6-diamino-2-methylsulfanylpyrimidinium Terafluoroborate (11·HBF$_4$). Yield: 82%. Mp 135−136 °C. Description: white solid. IR (KBr, cm^{-1}): ν = 3506, 3383, 2965, 2936, 1615, 1594, 1530, 1338, 1223, 1085 (BF_4^-), 776. HRMS *m*/*z* calcd for $C_9H_{16}N_4S$, 212.1090; found, 212.1072.

Acknowledgment. The authors are grateful to Gábor Czira for the HRMS measurements and to Béla Hegedus for the IR spectra. B.N. and T.V. acknowledge financial support from OTKA Grant T048796.

Supporting Information Available: Spectroscopic methods, computational methods, additional synthetic methods, NMR and IR spectra of the studied molecules, NPA charges, NICS indices, MEPs, chart of the correlation between ΔG in DMSO and ΔH in the gas phase, details of the calculation of temperature correction, Cartesian coordinates, and total energies. This material is available free of charge via the Internet at http://pubs.acs.org.

JO0605703